FACULTY OF ENGINEERING SCIENCE
DEPARTMENT OF MECHANICAL ENGINEERING
Beweging

KU LEUVEN

Beweging: project linkages

Matthias Derez, Andreas De Meester

2020-2021

Contents

List of Figures

1 Introduction

In this report a rod mechanism is analysed to get a better view on the kinematics and dynamics. The mechanism consists of 8 rods and 8 joints and can be used for a straight, parallel, horizontal movement. Another possibility is to let the mechanism move vertically, so it can be used as a lift. The joints are considered weightless and frictionless. The mechanism is shown in Figures 1 through 3. In this report, a kinematic and dynamic analysis are performed on the mechanism. The kinematic analysis calculates the position, velocities and acceleration of each rod. The dynamic analysis calculates the forces on each joint.

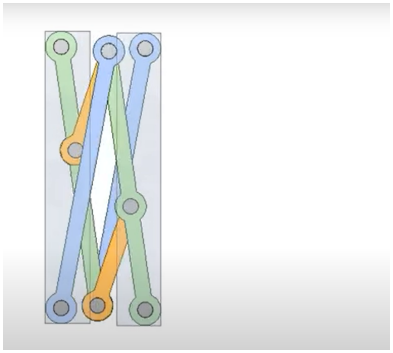

Figure 1: Mechanism in closed state

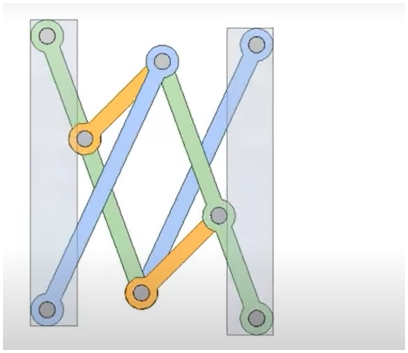

Figure 2: Mechanism in a semi open state

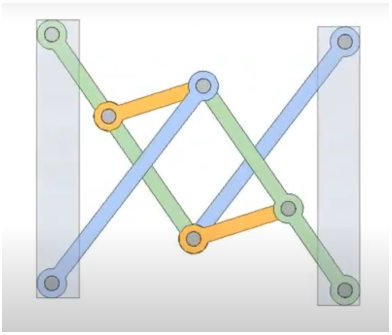

Figure 3: Mechanism in an open state

For this report, we used `MATLAB`. In particular, we made use of the following `MATLAB` scripts:

1. `start.m` the main program where all important functions are recalled.
2. `loopclosure_eqs.m` contains the loop closure equations.
3. `kinematics_4bar.m` contains the kinematic analysis and its control.
4. `dynamics_4bar.m` contains the dynamic analysis and its control.

1.1 Mobilty analysis

To determine the number of degrees of freedom (DOF), the mobility M of the mechanism is calculated. This can be done using Eq. 1, where n is the number of rods, f_1 is the number of joints who remove two DOF and f_2 the number of joints who remove one DOF.

$$M = 3(n-1) - 2f_1 - f_2 = 1 \tag{1}$$

The mechanism consists of 8 rods and 8 joints which remove 2 DOF. 2 of these joints are connected to 3 different rods so they need to be counted twice. This gives a mobility of $M = 1$.

1.2 Parameters

Figure 4 shows the diagram of the mechanism. The angles are always indicated from the positive x-axis, oriented counterclockwise. The report uses the same naming for each rod and joint throughout the report. The rods are numbered from 1 to 8, while the joints are numbered from A to H. The length and the naming of each rod can be seen in Table 1 where the naming corresponds to the naming of Figure 4.

Rod 1 remains still and is chosen as a reference. As no specifications were given to which rod is driven, the assumption was made that rod 2 is driven, or ϕ_2 is the driven angle. The goal of the motion is to keep rod 8 parallel to rod 1, while the mechanism unfolds. To calculate the mass of the rods, the following properties were used: $\rho = 7800\,\mathrm{kg/m^3}$ (steel), $A = 4\,\mathrm{cm}^2$. This gives a mass per unit length of $3.12\,\mathrm{kg/m}$.

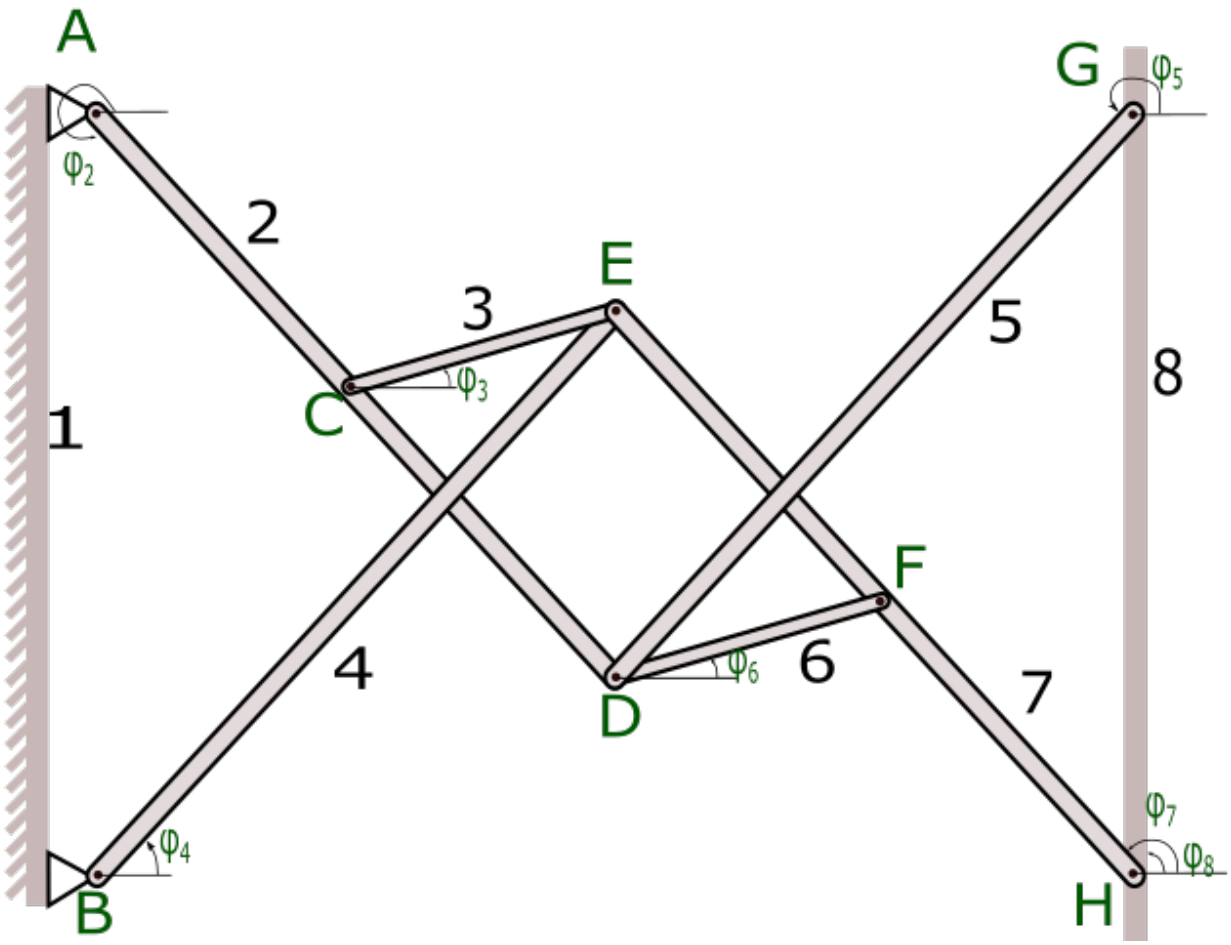

Figure 4: Mechanism with used parameters

1.3 Dead configurations

In theory, the mechanism has a dead configuration when $\phi_2 = 3\pi/2$. However, in practice ϕ_2 can never equal exactly $3\pi/2$ because of the thickness of the bars and joints. To prevent failure, ϕ_2 shouldn't be too large. This is why ϕ_2 is chosen to vary in the range of $3\pi/2+\pi/18$ to $3\pi/2+3\pi/18$.

2 Kinematic analysis

The joint being driven is joint A. The angle ϕ_2 can be separated into $3\pi/2+\phi_{2i}$, the starting angle, and a sinusoidal function where the sinusoidal function is driving the joint. By choosing the amplitude of the sinusoidal movement equal to $\phi_{2i}/2$, we avoid a dead point in both directions of the movement. The value of ϕ_{2i} can be found in Table 2. An angular velocity of $0.5 rad/s$ was applied. This angular velocity seems an appropriate magnitude to open and close the mechanism in a reasonable time. In the position $\phi_2 = 3\pi/2$, the mechanism is closed. An initial condition was added onto the initial angles of the joints. This is important to do because it determines which branch the mechanism is in. These numbers must be guessed and `MATLAB` will then calculate the correct angles.

The initial conditions for each rod can be found below. ε was added to the last equation to make sure this rod would be in the right quadrant.

$$\phi_2 = 3\pi/2+\phi_{2i}+\frac{\phi_{2i}}{2}sin(\omega t); \tag{2}$$

Table 1: Length and naming of the rods.

1	r_1	$\|AB\|$	$1m$
2	r_2	$\|AC\|$	$0.4m$
3	r_3	$\|CE\|$	$0.4m$
4	r_4	$\|BE\|$	$1m$
5	r_5	$\|DG\|$	$1m$
6	r_6	$\|DF\|$	$0.4m$
7	r_7	$\|HF\|$	$0.4m$
8	r_8	$\|HG\|$	$1m$
9	r_9	$\|CD\|$	$0.6m$
10	r_{10}	$\|EF\|$	$0.6m$

Table 2: Initial angles of joints.

1	ϕ_i	$\pi/9$
2	ϕ_{2i}	ϕ_i
3	ϕ_{3i}	ϕ_i
4	ϕ_{4i}	$\pi/2-\phi_i$
5	ϕ_{5i}	$\pi/2-\phi_i$
6	ϕ_{6i}	ϕ_i
7	ϕ_{7i}	$\pi/2+\phi_i$
8	ϕ_{8i}	$\pi/2-\varepsilon$

2.1 Position analysis

Tree independant loop equations can be found in the mechanism.

1. $A \rightarrow C \rightarrow E \rightarrow B$
2. $C \rightarrow E \rightarrow F \rightarrow D$
3. $G \rightarrow D \rightarrow F \rightarrow H$

The equations are split in a X and Y component where each equation must equal zero, to fulfil the condition that the loop is closed.

$$\text{Loop equation 1}: \begin{cases} \text{x: } r_1\cos(\phi_1) + r_2\cos(\phi_2) + r_3\cos(\phi_3) - r_4\cos(\phi_4) = 0 \\ \text{y: } r_1\sin(\phi_1) + r_2\sin(\phi_2) + r_3\sin(\phi_3) - r_4\sin(\phi_4) = 0 \end{cases} \tag{3}$$

$$\text{Loop equation 2}: \begin{cases} \text{x: } r_8\cos(\phi_8) + r_5\cos(\phi_5) + r_6\cos(\phi_6) - r_7\cos(\phi_7) = 0 \\ \text{y: } r_8\sin(\phi_8) + r_5\sin(\phi_5) + r_6\sin(\phi_6) - r_7\sin(\phi_7) = 0 \end{cases} \tag{4}$$

$$\text{Loop equation 3}: \begin{cases} \text{x: } r_3\cos(\phi_3) - r_{10}\cos(\phi_7) - r_6\cos(\phi_6) - r_9\cos(\phi_2) = 0 \\ \text{y: } r_3\sin(\phi_3) - r_{10}\sin(\phi_7) - r_6\sin(\phi_6) - r_9\sin(\phi_2) = 0 \end{cases} \tag{5}$$

The resulting assembly provided by the `MATLAB` script can be seen in Figure 5. The angles of each bar in function of time can be seen in Figure 6. Angle ϕ_8 deserves some more attention, it remains almost entirely constant at an angle of $\pi/2$. This is enlarged in Figure 7. The variation in this angle is approximately than $10^{-11} rad$. This angle is related to rod 8, and the purpose of this mechanism is to horizontally move rod 8, while the rod itself stays in a vertical position. Hereby is this successful in it's intent. The fact that machine precision isn't achieved can be be explained by the fact that the angle is derived using the *fsolve* command. By adjusting the convergence criteria in this command, the deviation from $\pi/2$ can be lowered, although it becomes harder to find convergence.

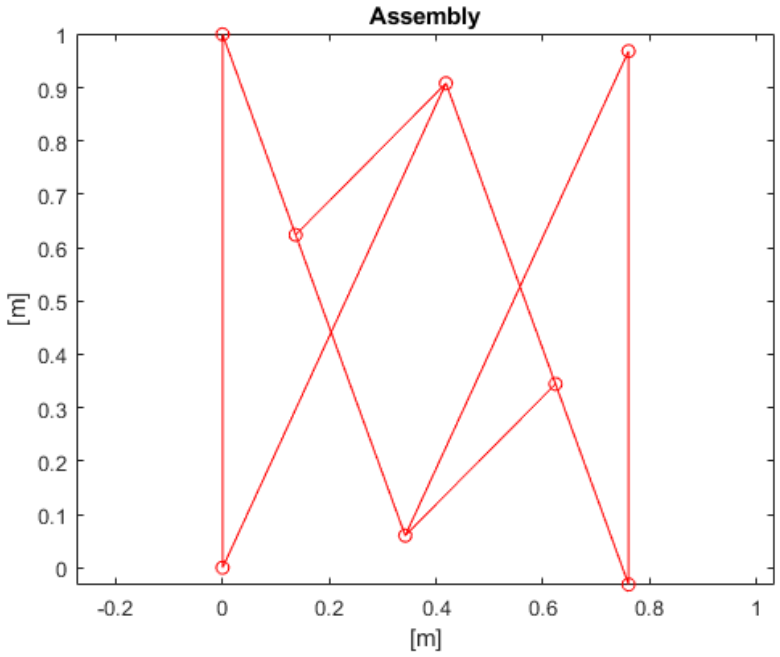

Figure 5: Assembly of the mechanism

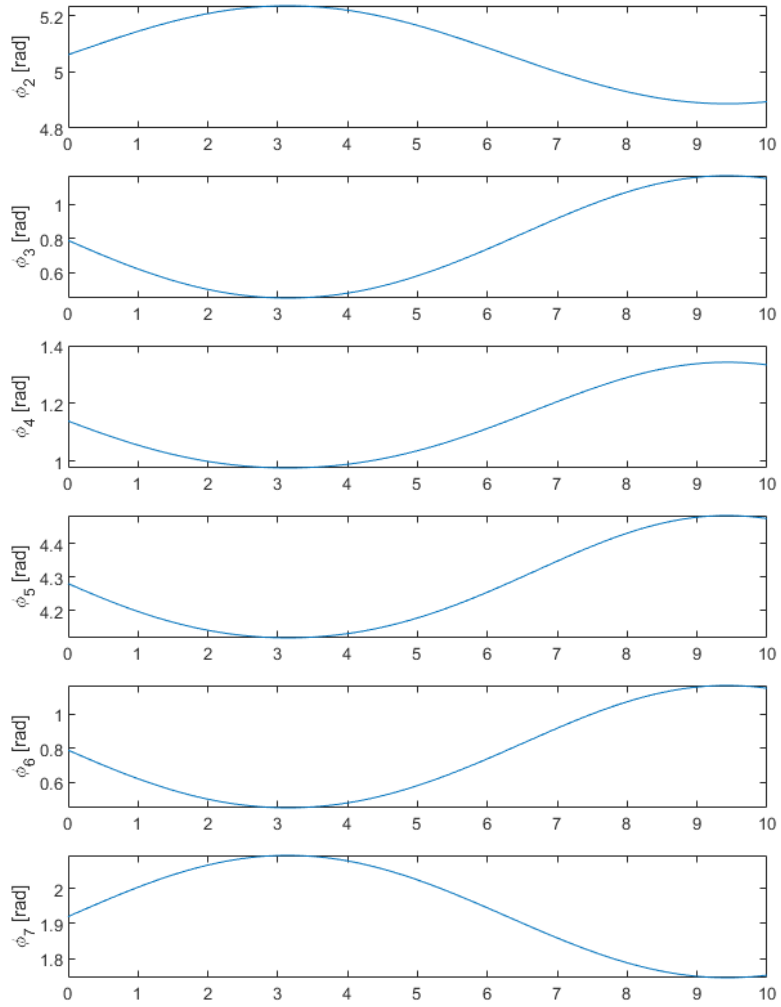

Figure 6: Angles of each joint in function of time.

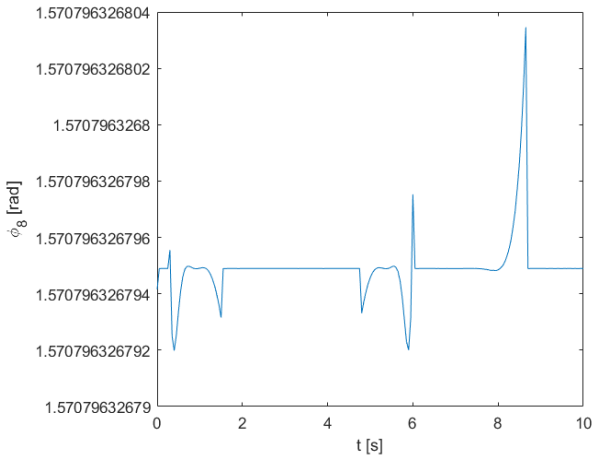

Figure 7: ϕ_8 in function of time.

2.2 Velocity analysis

Next, the velocity analysis will be discussed. The time derivative of the loop equations are the kinematic equations. This responds in following matrices:

$$A_m \cdot X = B_m \tag{6}$$

$$A_m = \begin{pmatrix} -r_3\sin(\phi_3(k)) & r_4\sin(\phi_4(k)) & 0 & 0 & 0 & 0 \\ r_3\cos(\phi_3(k)) & -r_4\cos(\phi_4(k)) & 0 & 0 & 0 & 0 \\ 0 & 0 & -r_5\sin(\phi_5(k)) & -r_6\sin(\phi_6(k)) & r_7\sin(\phi_7(k)) & -r_8\sin(\phi_8(k)) \\ 0 & 0 & r_5\cos(\phi_5(k)) & r_6\cos(\phi_6(k)) & -r_7\cos(\phi_7(k)) & r_8\cos(\phi_8(k)) \\ -r_3\sin(\phi_3(k)) & 0 & 0 & r_6\sin(\phi_6(k)) & r_{10}\sin(\phi_7(k)) & 0 \\ r_3\cos(\phi_3(k)) & 0 & 0 & -r_6\cos(\phi_6(k)) & -r_{10}\cos(\phi 7(k)) & 0 \end{pmatrix}$$

(7)

$$B_m = \begin{pmatrix} r_2\sin(\phi_2(k))\,d\phi_2(k) \\ -r_2\cos(\phi_2(k))\,d\phi_2(k) \\ 0 \\ 0 \\ -r_9\sin(\phi_2(k))\,d\phi_2(k) \\ r_9\cos(\phi_2(k))\,d\phi_2(k) \end{pmatrix} \tag{8}$$

The result calculated from Equation 6 is shown in Figure 8. In this Figure, some things can be noticed. The angular velocity of rod 8: $d\phi_8$ is almost entirely equal to zero, apart from one small deviation. The variation however is very small, less then $4 \cdot 10^{-12} rad/s$. This variation can be blamed to the little variations in ϕ_8 itself, as explained in Section 2.1.

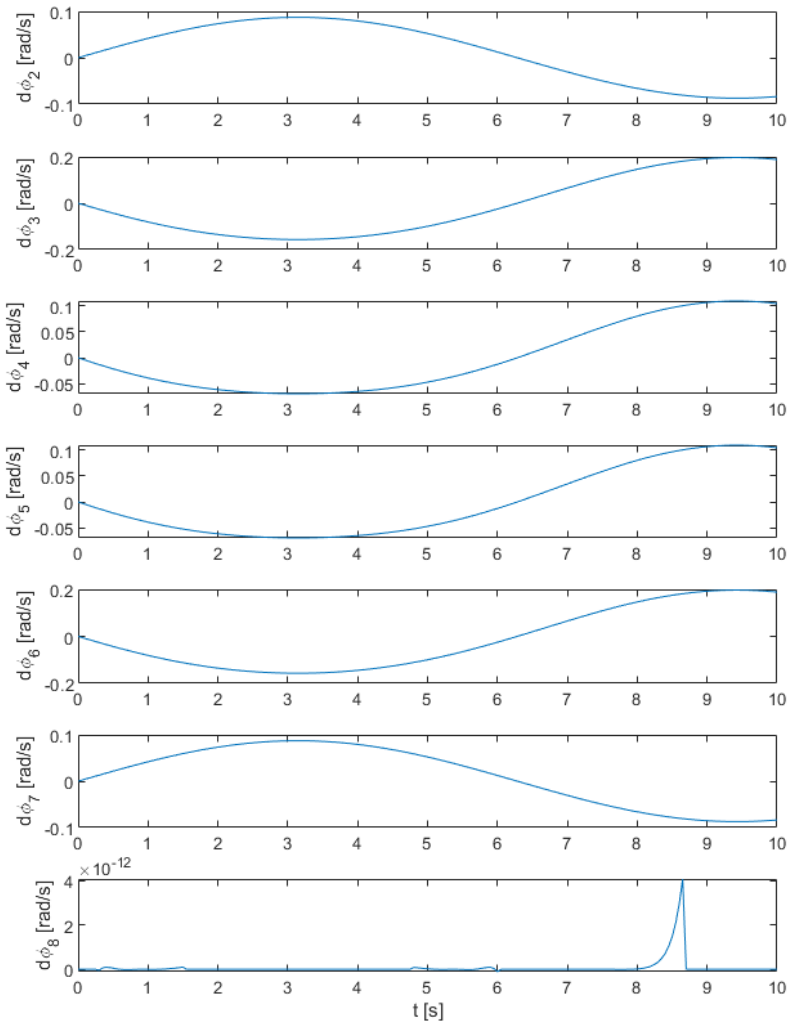

Figure 8: Angular velocity of each joint.

2.3 Acceleration analysis

The calculation of the acceleration is similar to the calculation of the velocity. Equation 9 must be solved. We calculate matrix A and B by taking the derivative of the equations used in the velocity analysis.

$$A \cdot X = B \tag{9}$$

This gives the following matrices:

$$A = \begin{pmatrix} -r_3\sin(\phi_3(k)) & r_4\sin(\phi_4(k)) & 0 & 0 & 0 & 0 \\ r_3\cos(\phi_3(k)) & -r_4\cos(\phi_4(k)) & 0 & 0 & 0 & 0 \\ 0 & 0 & -r_5\sin(\phi_5(k)) & -r_6\sin(\phi_6(k)) & r_7\sin(\phi_7(k)) & -r_8\sin(\phi_8(k)) \\ 0 & 0 & r_5\cos(\phi_5(k)) & r_6\cos(\phi_6(k)) & -r_7\cos(\phi_7(k)) & r_8\cos(\phi_8(k)) \\ -r_3\sin(\phi_3(k)) & 0 & 0 & r_6\sin(\phi_6(k)) & r_{10}\sin(\phi_7(k)) & 0 \\ r_3\cos(\phi_3(k)) & 0 & 0 & -r_6\cos(\phi_6(k)) & -r_{10}\cos(\phi_7(k)) & 0 \end{pmatrix} \tag{10}$$

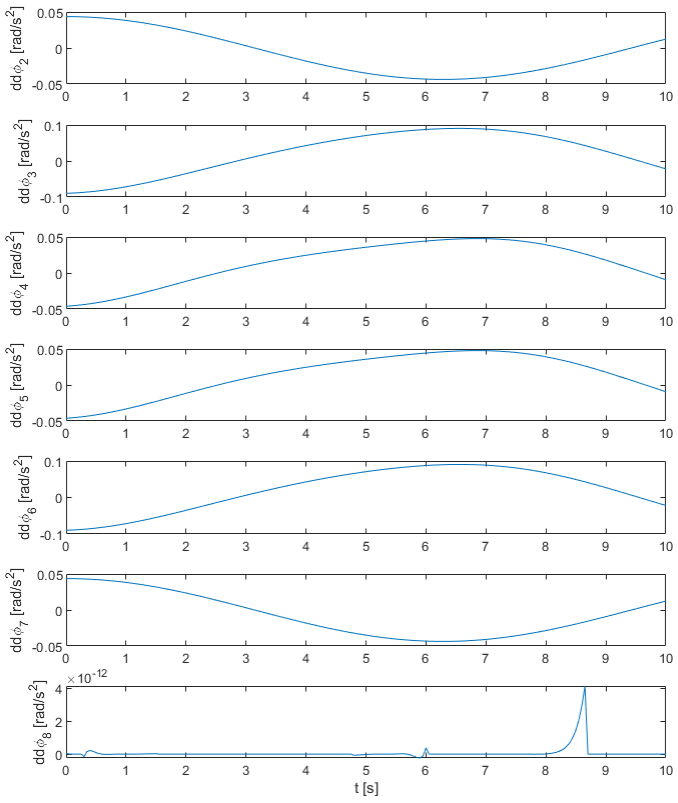

Figure 9: Angular acceleration of joints.

$$B = \begin{pmatrix} r_2\cos(\phi_2(k))\,d\phi_2(k)^2 + r_2\sin(\phi_2(k))\,dd\phi_2(k) + r_3\cos(\phi_3(k))\,d\phi_3(k)^2 - r_4\cos(\phi_4(k))\,d\phi_4(k)^2 \\ r_2\sin(\phi_2(k))\,d\phi_2(k)^2 - r_2\cos(\phi_2(k))\,dd\phi_2(k) + r_3\sin(\phi_3(k))\,d\phi_3(k)^2 - r_4\sin(\phi_4(k))\,d\phi_4(k)^2 \\ r_5\cos(\phi_5(k))\,d\phi_5(k)^2 + r_6\cos(\phi_6(k))\,d\phi_6(k)^2 - r_7\cos(\phi_7(k))\,d\phi_7(k)^2 + r_8\cos(\phi_8(k))\,d\phi_8(k)^2 \\ r_5\sin(\phi_5(k))\,d\phi_5(k)^2 + r_6\sin(\phi_6(k))\,d\phi 6(k)^2 - r_7\sin(\phi_7(k))\,d\phi_7(k)^2 + r_8\sin(\phi_8(k))\,d\phi_8(k)^2 \\ -r_9\cos(\phi_2(k))\,d\phi_2(k)^2 - r_9\sin(\phi_2(k))\,dd\phi_2(k) + r_3\cos(\phi 3(k))\,d\phi_3(k)^2 - r_6\cos(\phi_6(k))\,d\phi_6(k)^2 - r_{10}\cos(\phi_7(k))\,d\phi_7(k)^2 \\ -r_9\sin(\phi_2(k))\,d\phi_2(k)^2 + r_9\cos(\phi_2(k))\,dd\phi_2(k) + r_3\sin(\phi_3(k))\,d\phi_3(k)^2 - r_6\sin(\phi_6(k))\,d\phi_6(k)^2 - r_{10}\sin(\phi_7(k))\,d\phi_7(k)^2 \end{pmatrix} \tag{11}$$

When X is calculated from Equation 9, the angular acceleration can be seen in Figure 9. Logically, the acceleration from ϕ_8 is almost zero. The difference can once again be blaimed on the little deviations of ϕ_8 from $\pi/2$.

2.4 Control of kinematics

As the data found in the kinematic analysis is used in the inverse dynamic analysis, it is very important this data is correct. In the following paragraphs, the values found in the kinematic analysis are verified. Four ways of controlling are used. The first, most obvious way to control if the position analysis is correct, is graphically, by watching the animation. As the animation exactly depicts the movement of our mechanism, our program passes the first test. Next to that, the values of each angular velocity can be checked on sign. On first sight, the values also seem to pass this test. The third way is by calculating the position, velocity and acceleration of a point, using two different paths. The fourth method is an analytical approach, based on geometrical insight. These last two are further elaborated.

2.4.1 Method via separate paths

In this method, the position, velocity and acceleration of point F (see Figure 4), via two different paths. The data found via the two paths is then compared to each other and the absolute and relative errors are calculated.

Position analysis The paths used to calculate the position of point F are:

- Path 1: $\overrightarrow{AD} + \overrightarrow{DF}$
- Path 2: $\overrightarrow{AC} + \overrightarrow{CE} + \overrightarrow{EF}$

The positions found via the two paths can be seen in Figure 10. The absolute and relative errors can be found in Figure 11. As the errors are of magnitude $10^{-12}m$, we can conclude the position is calculated correct.

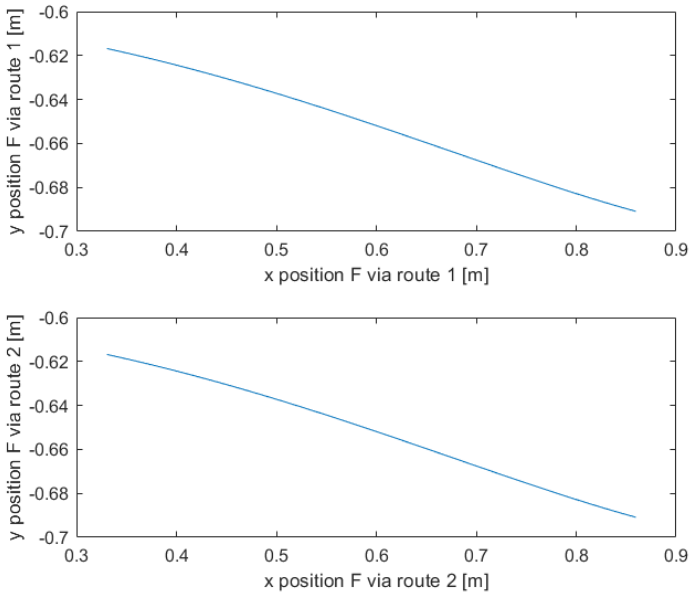

Figure 10: Control position F via 2 paths

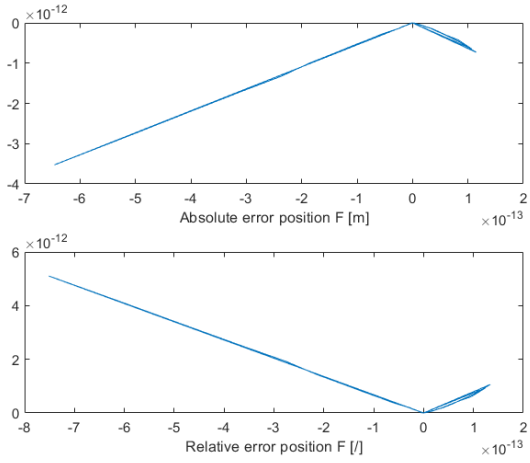

Figure 11: Errors position F via 2 paths

Velocity analysis Using the same two paths as in the position analysis, the velocity of F is calculated. For the first path, the velocities are calculated as follows:

$$v_D = \omega_2 \times \overrightarrow{AD}$$
$$v_F = v_D + \omega_6 \times \overrightarrow{DF}$$

For the second path, velocities are calculated in the following way:

$$v_C = \omega_2 \times \overrightarrow{AC}$$
$$v_E = v_C + \omega_3 \times \overrightarrow{CE}$$
$$v_F = v_E + \omega_7 \times \overrightarrow{EF}$$

The resulting velocities are shown in Figure 12 and Figure 14. The errors can be found in Figure 13 and Figure 15. As the errors have the magnitude of machine precision, we can conclude the velocities are calculated correctly.

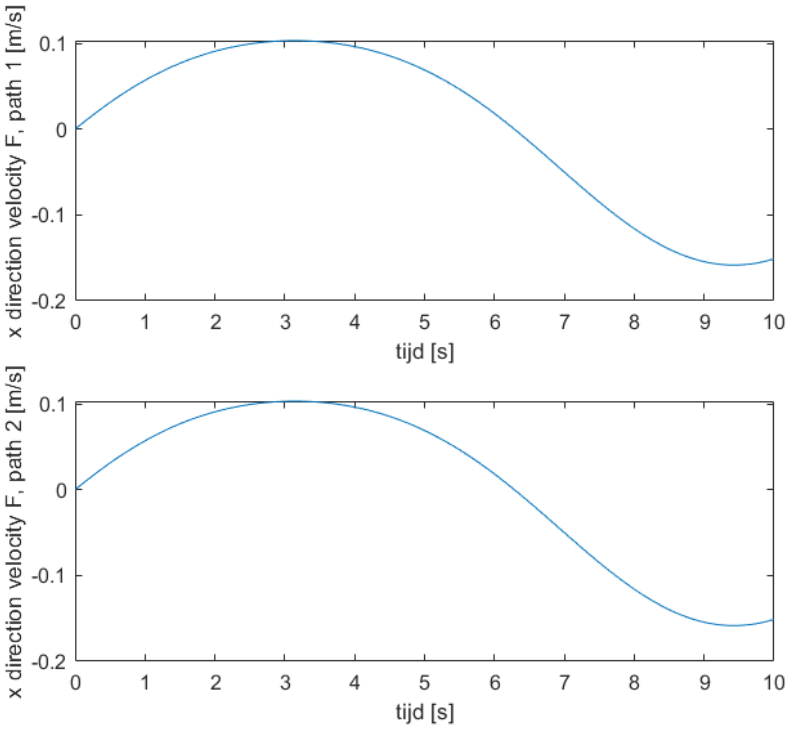

Figure 12: Control x direction velocity F via 2 paths

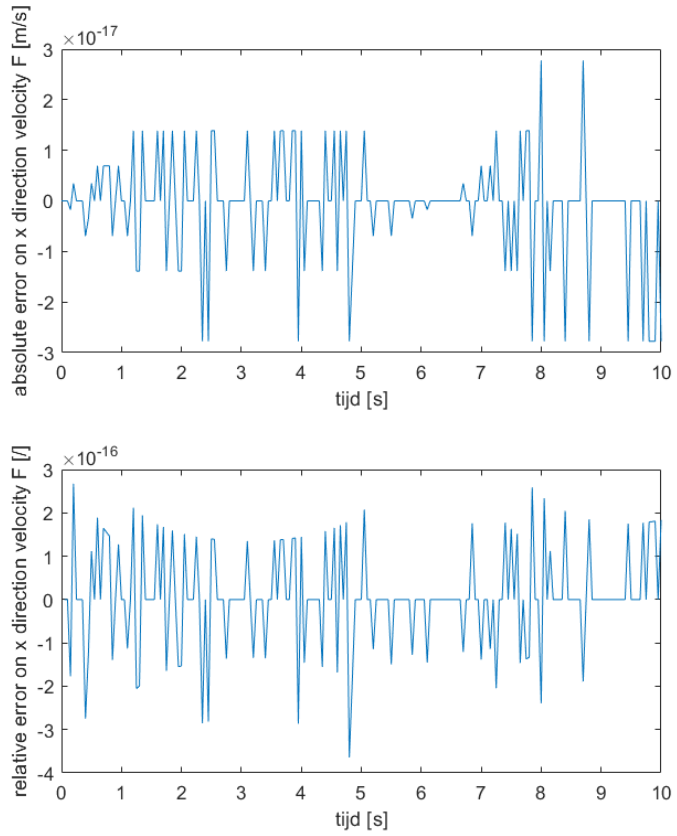

Figure 13: Errors x direction velocity F via 2 paths

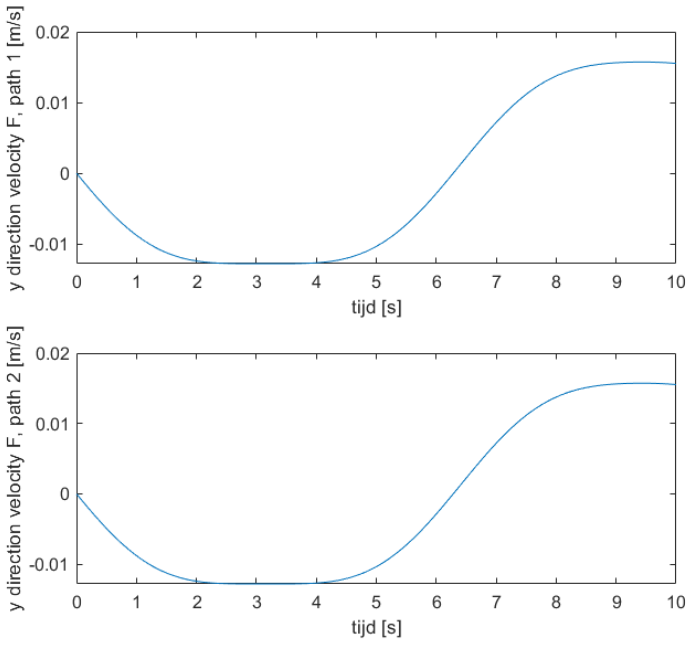

Figure 14: Control y direction velocity F via 2 paths

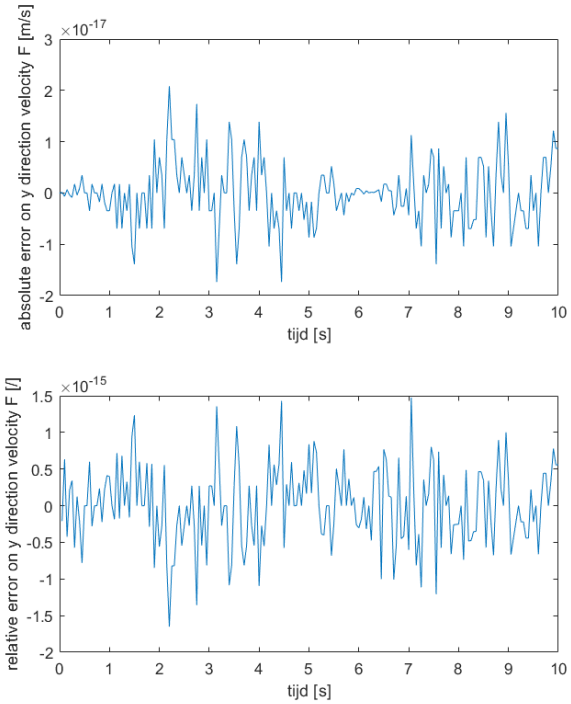

Figure 15: Errors y direction velocity F via 2 paths

Acceleration analysis Once again, the same two paths are used to calculate the acceleration of point F. For the first path, the accelerations are calculated as follows:

$$a_D = \omega_2 \times \omega_2 \times \overrightarrow{AD} + \alpha_2 \times \overrightarrow{AD}$$
$$a_F = a_D + \omega_6 \times \omega_6 \times \overrightarrow{DF} + \alpha_6 \times \overrightarrow{AD}$$

For the second path, accelerations are calculated in the following way:

$$a_C = \omega_2 \times \omega_2 \times \overrightarrow{AC} + \alpha_2 \times \overrightarrow{AC}$$
$$a_E = a_C + \omega_3 \times \omega_3 \times \overrightarrow{CE} + \alpha_3 \times \overrightarrow{CE}$$
$$a_F = a_E + \omega_7 \times \omega_7 \times \overrightarrow{EF} + \alpha_7 \times \overrightarrow{EF}$$

The calculated accelerations of point F can be found in Figure 16 and Figure 18. The absolute and relative errors between the accelerations found using the two paths are shown in Figure 17 and Figure 19. Again, as the magnitude of these errors is close to machine precision, we can conclude the accelerations are calculated correctly.

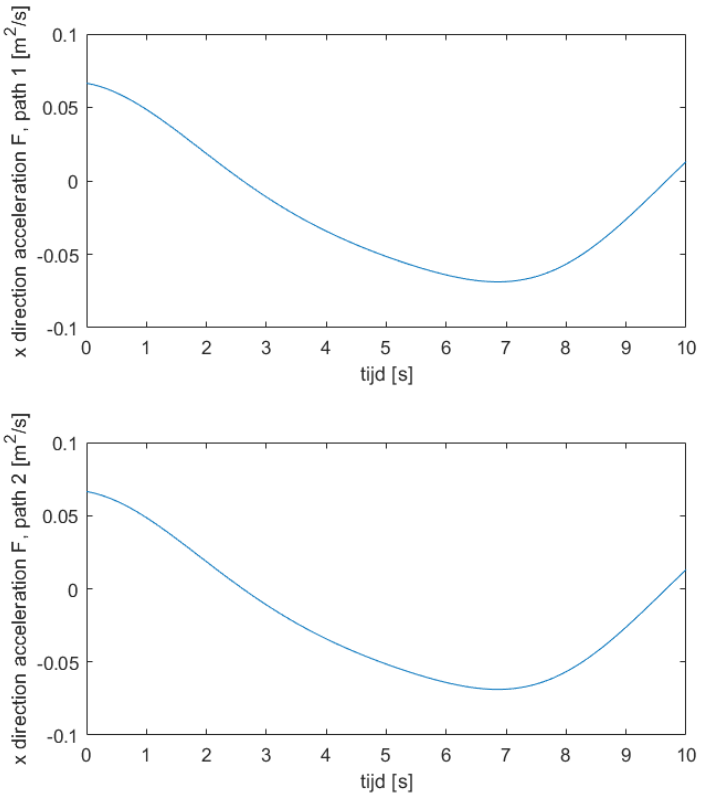

Figure 16: Control x direction acceleration F via 2 paths

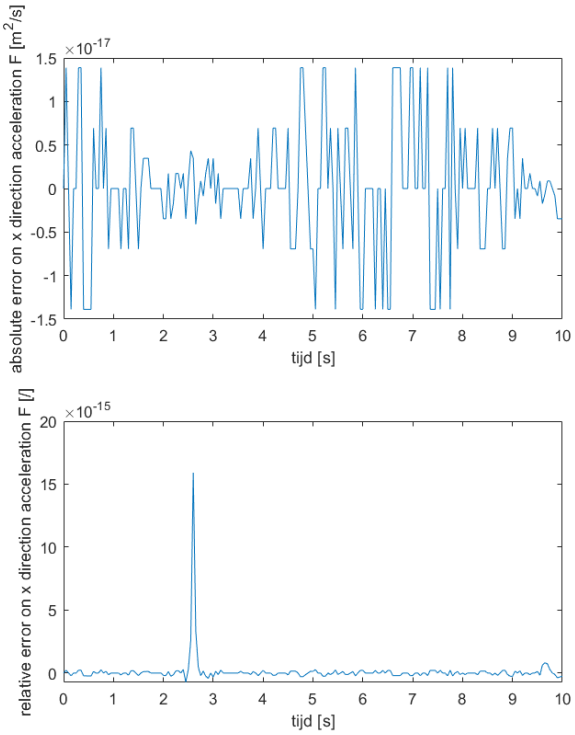

Figure 17: Errors x direction acceleration F via 2 paths

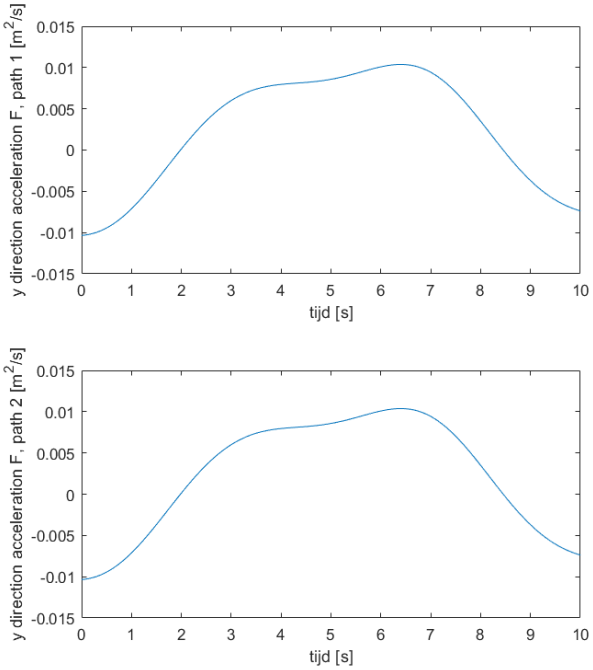

Figure 18: Control y direction acceleration F via 2 paths

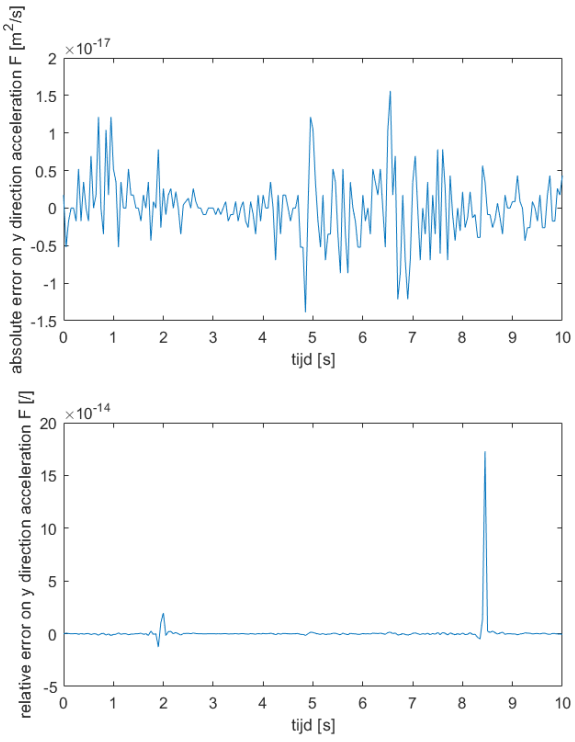

Figure 19: Errors y direction acceleration F via 2 paths

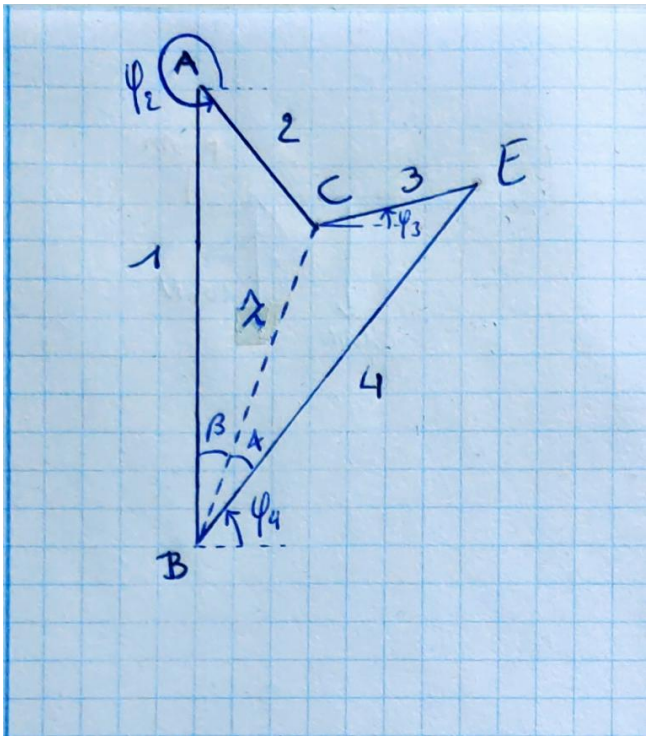

Figure 20: Parameters used in control based on geometrical insight

2.4.2 Method based on geometrical insight

Another control can be done by an analytic approach based on geometrical insight. We used an ad hoc method based on slide $10-18$ of Lecture 2 of the course Beweging en Trillingen: beweging.

Position analysis By performing a control on loop *ACEB* based on geometrical insight, we can verify angles ϕ_3 and ϕ_4. Using Figure 20 the following equations can be drawn up:

$$z^2 = r_1^2 + r_2^2 - 2r_1 r_2 * \cos\phi_2 \tag{12}$$

$$\alpha = \arccos\frac{r_3^2 - z^2 - r_4^2}{-2r_4 z} \tag{13}$$

$$\beta = \arccos\frac{r_2^2 - z^2 - r_1^2}{-2r_1 z} \tag{14}$$

From Equation 12 to 14, ϕ_3 can be derived.

$$\phi_4 = \pi/2 - \alpha - \beta \tag{15}$$

From Equation 16, ϕ_3 can be derived as in Equation 17:

$$r_4^2 = z^2 + r_3^2 - 2zr_3 cos(\beta + \pi/2 + \phi_3) \tag{16}$$

$$\phi_3 = -\beta - \pi/2 + \arccos\frac{r_4^2 - z^2 - r_3^2}{-2rz_3} \tag{17}$$

In Figure 21, the result can be seen, where ϕ_4 is the angle calculated in the position analysis and ϕ_{4c} the angle calculated in our control method. The difference is in the order of $10^{-13} rad$ which suggests the calculations are done correctly.

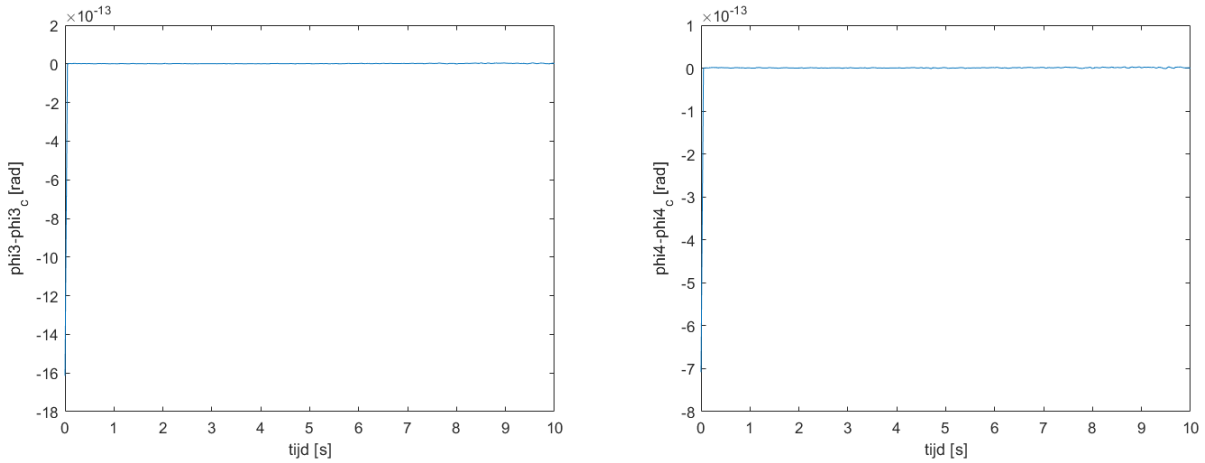

Figure 21: Control of ϕ_3 and ϕ_4

Velocity analysis Starting from Equations 18, 19 and 20, Equation 21 can be derived.

$$v_C = \omega_2 \times \overrightarrow{AC} \tag{18}$$

$$v_E = \omega_4 \times \overrightarrow{BE} \tag{19}$$

$$v_E = v_C + \omega_3 \times \overrightarrow{CE} \tag{20}$$

$$\omega_4 \times \overrightarrow{BE} = \omega_2 \times \overrightarrow{AC} + \omega \times \overrightarrow{CE} \tag{21}$$

By expressing Equation 21 in the x and y direction, Equations 23 and 22 are found. In these expressions, r_{4y} for example is linked to the y component of r_4. If these components are expressed as functions of sin or cos of the given angles, Equations 22 and 22 are found, which are the exact same expressions as those used in Section 2.2. This shows us the expressions used in that section are correct.

$$r_{4x}\omega_4 = r_{2x}\omega_2 + r_{3x}\omega_3 \tag{22}$$

$$-r_{4y}\omega_4 = -r_{2y}\omega_2 - r_{3y}\omega_3 \tag{23}$$

Acceleration analysis Analogue to the equations on slide 17, Lecture 2 of Beweging en Trillingen: beweging, Equations 24 to 26 can be written down.

$$a_C = \omega_2 \times \omega_2 \times \overrightarrow{AC} + \alpha_2 \times \overrightarrow{AC} \tag{24}$$

$$a_E = \omega_4 \times \omega_4 \times \overrightarrow{BE} + \alpha_4 \times \overrightarrow{BE} \tag{25}$$

$$a_E = a_C + \omega_3 \times \omega_3 \times \overrightarrow{CE} + \alpha_3 \times \overrightarrow{CE} \tag{26}$$

Combining these equations, Equation 27 can be found. Expressing this equation in the x and y direction gives Equations 28 and 29.

$$\omega_4 \times \omega_4 \times \overrightarrow{BE} + \alpha_4 \times \overrightarrow{BE} = \omega_2 \times \omega_2 \times \overrightarrow{AC} + \alpha_2 \times \overrightarrow{AC} + \omega_3 \times \omega_3 \times \overrightarrow{CE} + \alpha_3 \times \overrightarrow{CE} \tag{27}$$

$$-r_{4y}\alpha_4 + acc_{4x} = -r_{2y}\alpha_4 + acc_{2x} - r_{3y}\alpha_3 + acc_{3x} \tag{28}$$

$$r_{4x}\alpha_4 + acc_{4y} = r_{2x}\alpha_2 + acc_{2y} + r_{3x}\alpha_3 + acc_{3y} \tag{29}$$

These equations can be solved in `MATLAB`, yielding values for $dd\phi_3$ and $dd\phi_4$. The relative errors of the results are shown in Figure 22. Here $dd\phi_3$ stands for the value found in the kinematic analysis and α_{3c} stands for the value found in the control. As the relative error is of the order of magnitude of $10^{-14} rad/s^2$, we can conclude the calculations are correct.

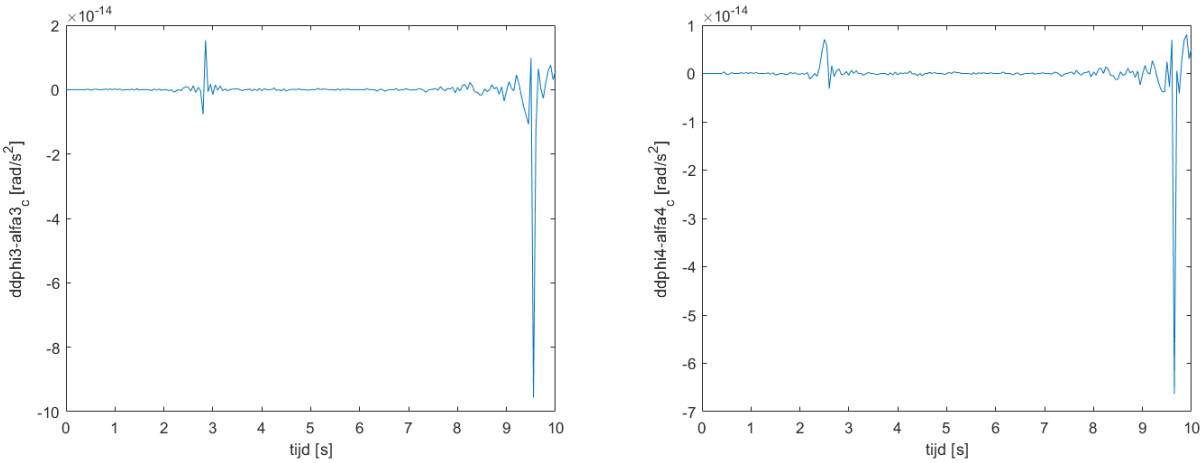

Figure 22: Relative errors on acceleration control

3 Inverse dynamic analysis

Making use of the results found in the kinematic analysis, an inverse dynamic analysis can be done. The center of gravity (COG) lays in the middle of each rod. A new coordinate system was introduced for each bar. The X axis lays along the direction of the rod and the Y axis perpendicular to the rod with the center of the coordinate system in the COG. This results in the fact that the joints all have the coordinates ($\pm$ length of the rod/2, 0). The y-coordinate is always zero, as the joints lay on the same height as the COG in this new coordinate system. This actually isn't fully correct for bar 1 and 8. As can be seen in Figure 3, the joints aren't positioned perfectly in the middle of these bars. As this deviation is only small and the mechanism wouldn't work differently if the joints were positioned in the middle, this small error is neglected.

3.1 Free body diagrams

The first step in the inverse dynamic analysis is drawing the free body diagrams. These can be found in Figure 23 and Figure 24. Each bar provides 3 equations: the force equilibrium in the x-direction, the force equilibrium in the y-direction and the momentum equilibrium. Applying this to bars two through eight, 21 equations can be found. As there are are 20 unknown forces and 1 unknown moment, this is a solvable system. The abbreviation *cog*2*Ay* used in Figure 23 and 24 stands for the vertical distance from the centre of gravity of bar 2 to joint A. Analog reasoning applies to other bars and joints, with the x in the end denoting the horizontal distance. The moments are chosen positive in the counterclockwise direction. The symbol J_2 stands for the moment of inertia of bar 2 around its centre of gravity.

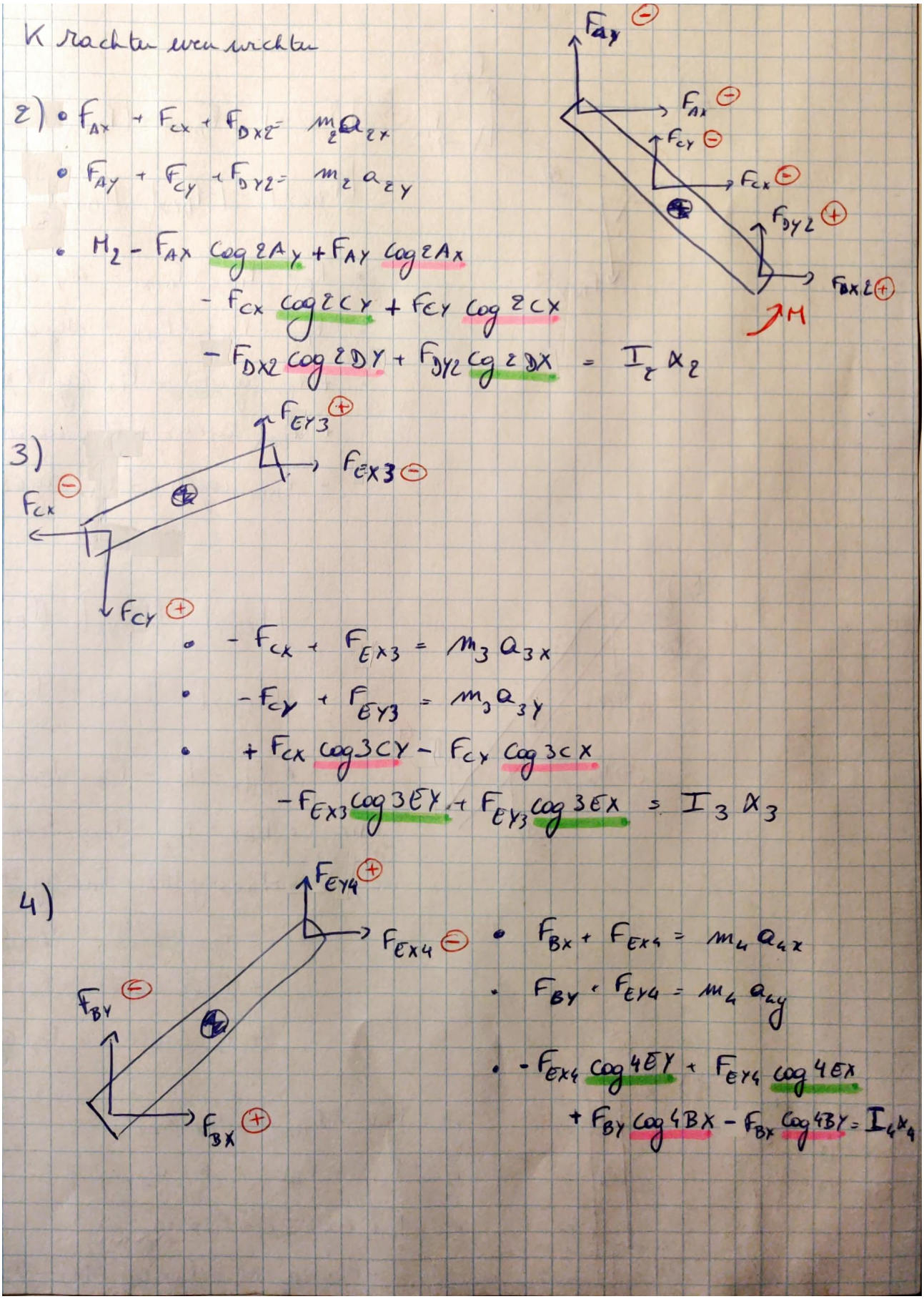

Figure 23: Free body diagram 1

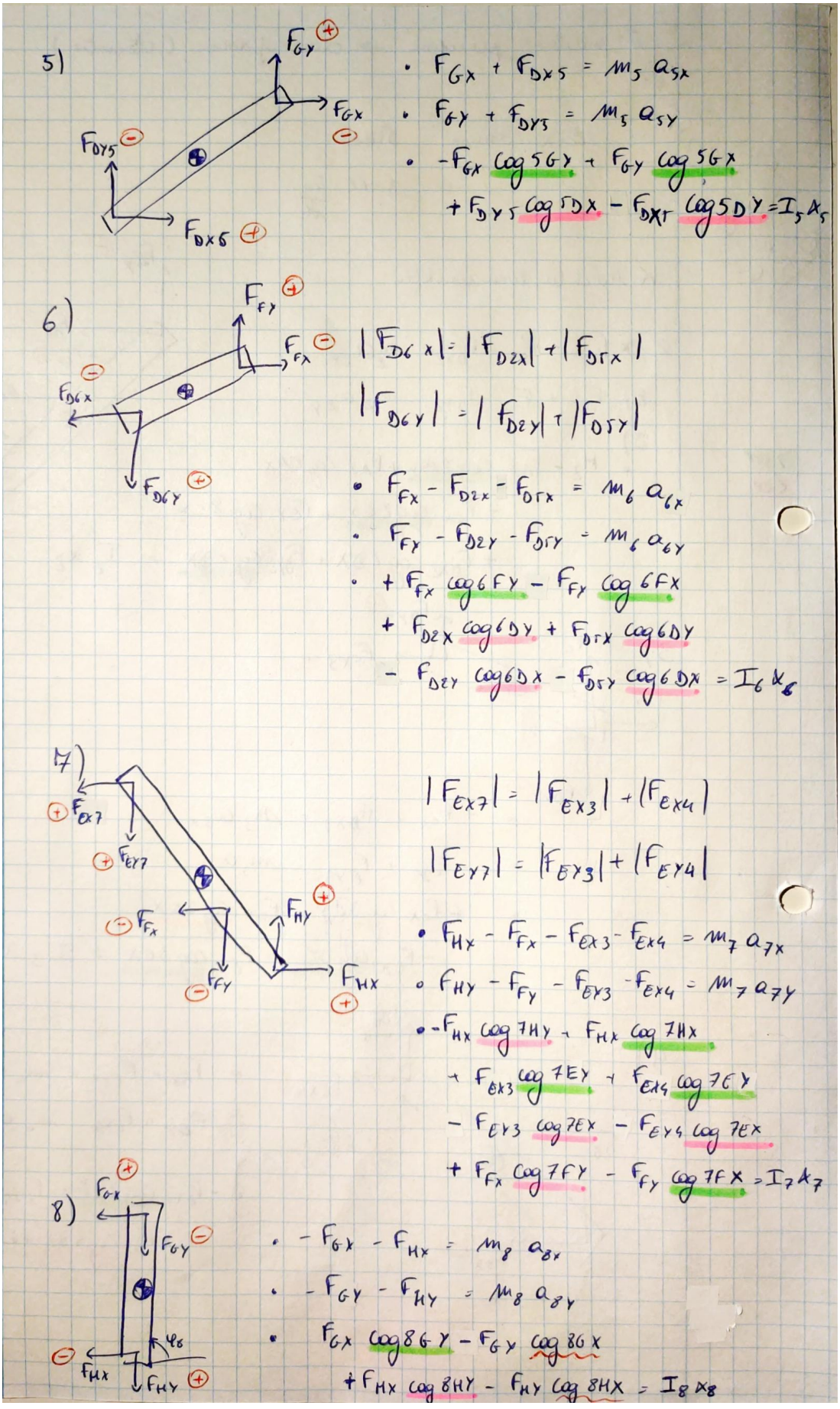

Figure 24: Free body diagram 2

3.2 Matrix method

The equations are written in the form of $A \cdot x = B$, where x is an $21x1$ column vector, containing the searched forces and moment. B is also an $21x1$ column vector, containing the elements of the the right-hand side of the equilibrium equations. A is an $21x21$ matrix, containing the coefficients of the equilibrium equations.

This equation can easily be solved in `MATLAB`, yielding the searched forces and moment in function of time. The results can be found in Figure 25 through Figure 29.

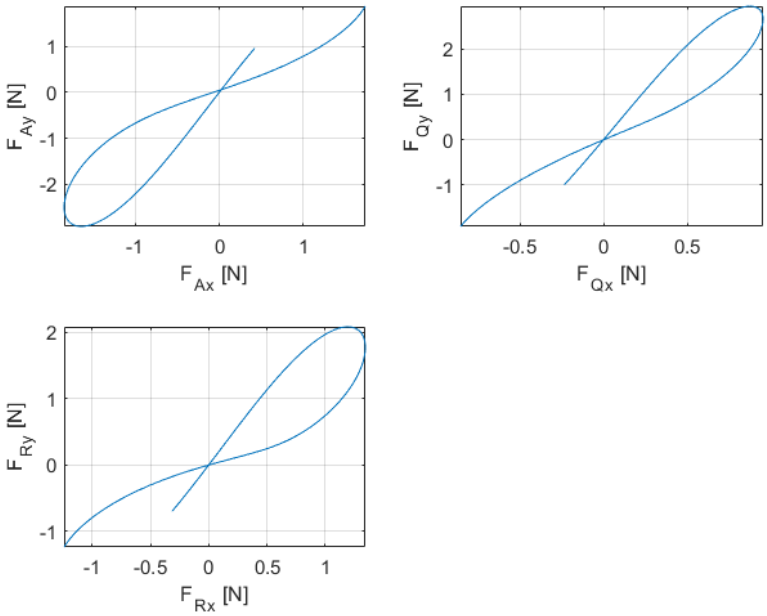

Figure 25: Forces in points A, Q and R

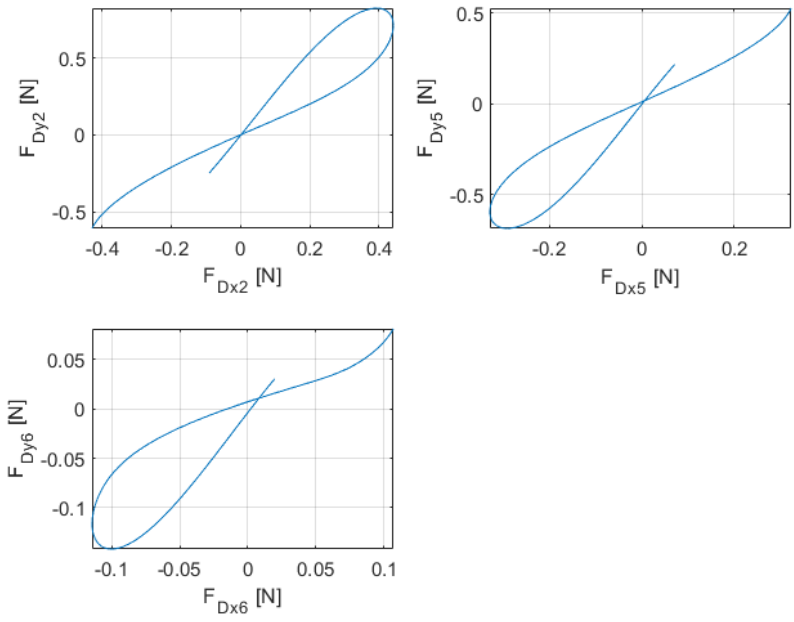

Figure 26: Forces in point D

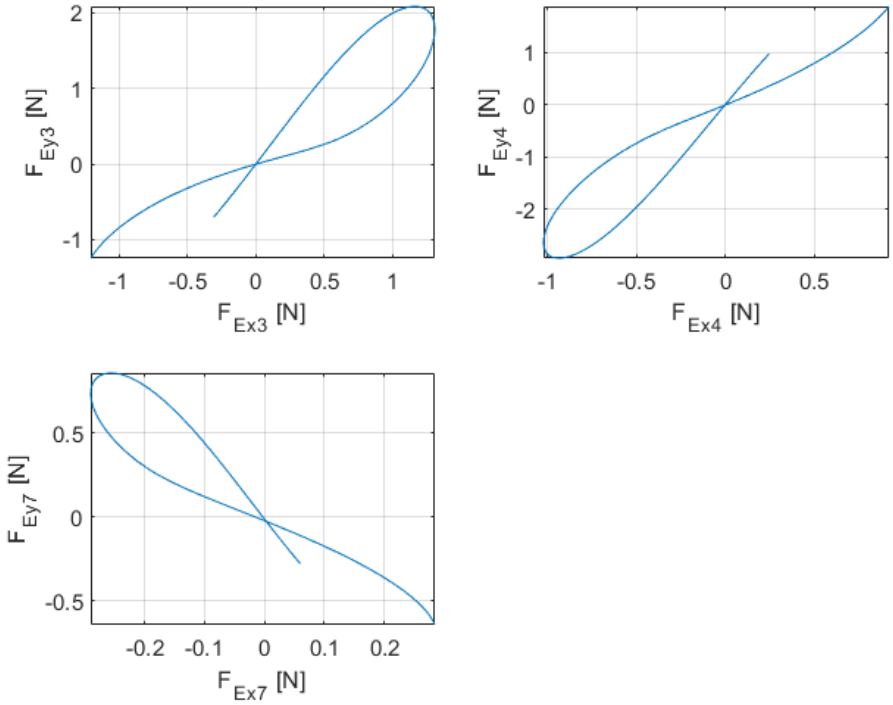

Figure 27: Forces in point E

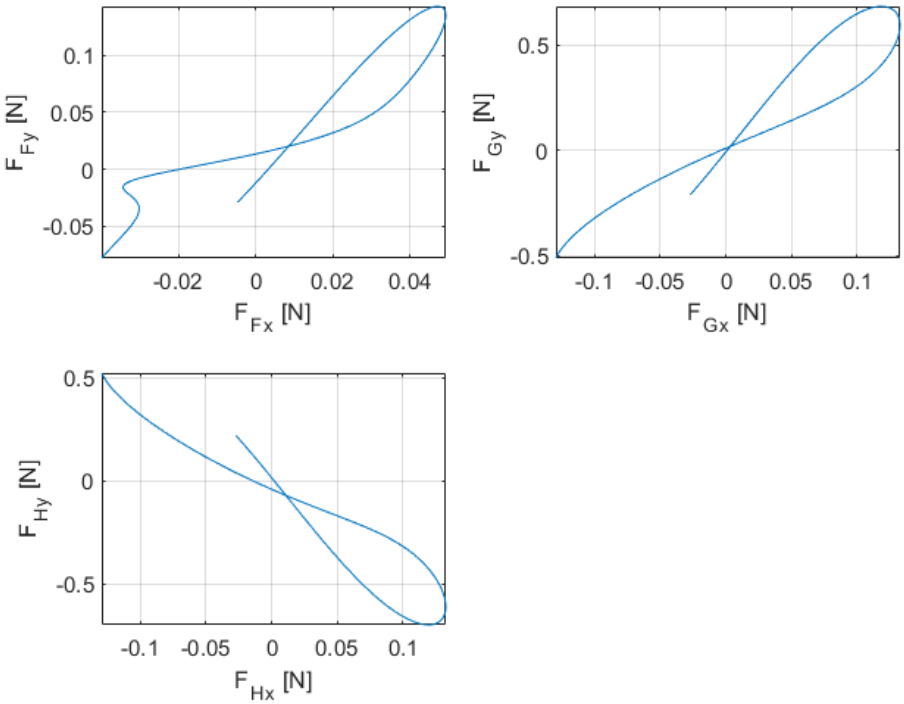

Figure 28: Forces in points F, G and H

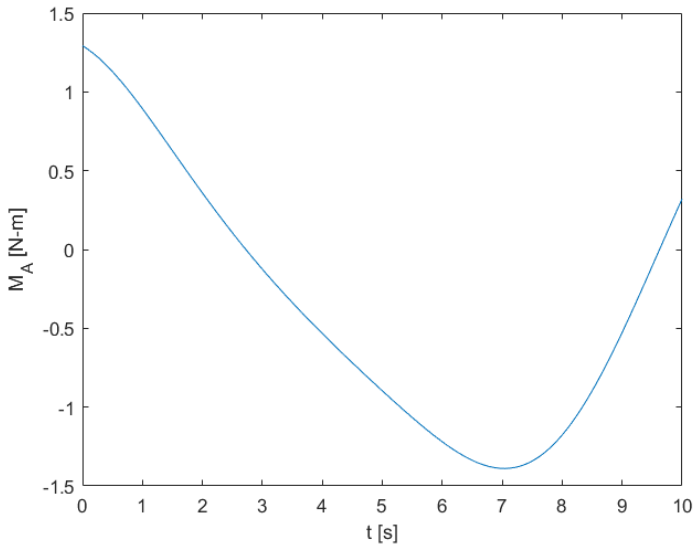

Figure 29: Driving moment M_A

3.3 Control: variation of kinetic energy

The method of variation of kinetic energy can be used for purely inertial systems and tells us the change in total kinetic energy equals power supplied by the driving forces. In our case, this yields in equation 30, where $v_i, a_i, \omega_i, \alpha_i$ are vectors.

$$M_{controle} = \frac{\sum_{i=2}^{8} m_i \cdot (v_i \cdot a_i) + I_{cogi} \cdot (\omega_i \cdot \alpha_i)}{\omega} \tag{30}$$

Solving this equation leads to $M_{controle}$, which can be found in Figure 30. In Figure 30, the difference between the two calculated driving moments is shown. As this is in the order of magnitude of machineprecision, we can conclude the control shows us that the calculated values for M_A are correct.

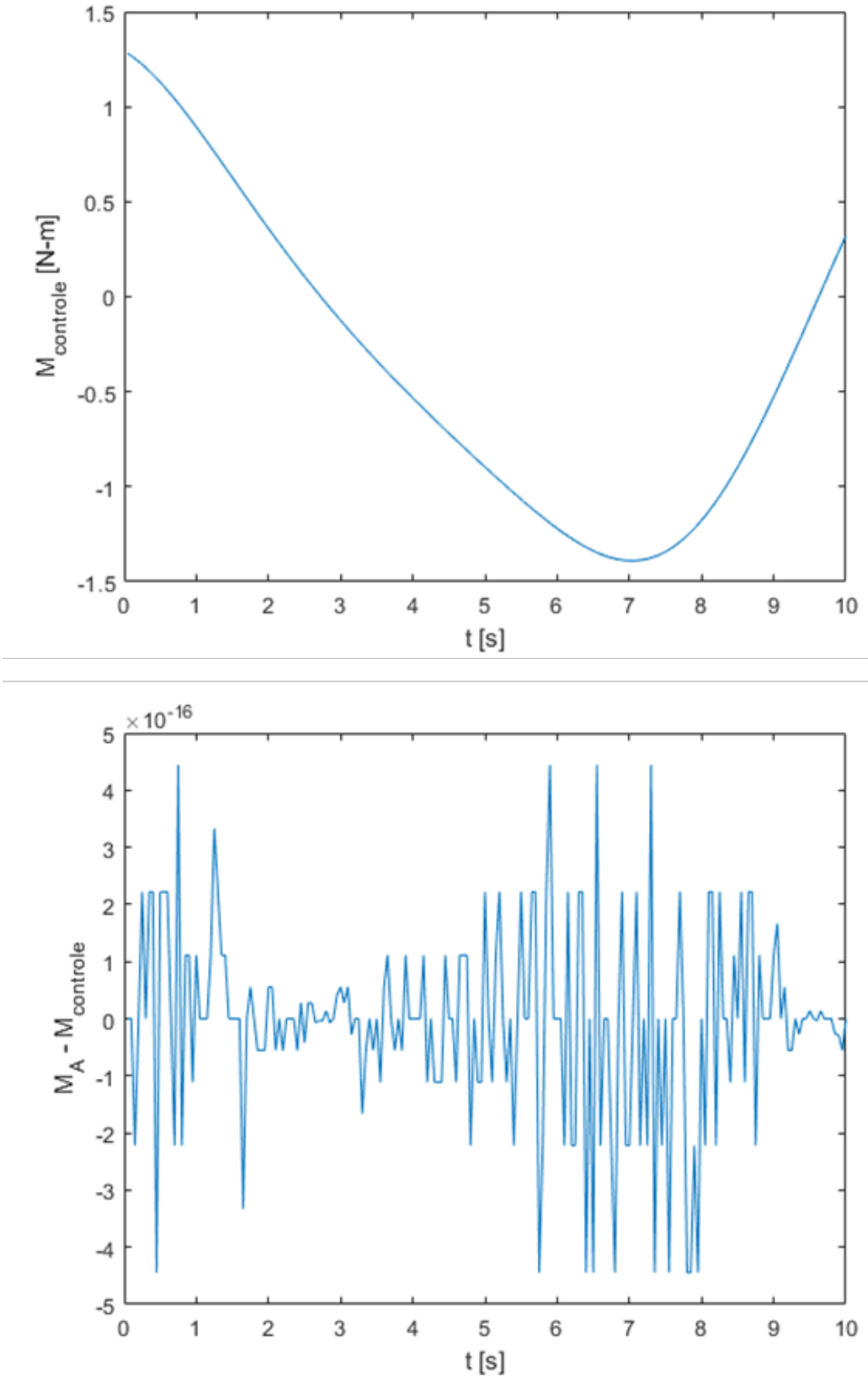

Figure 30: Control of driving moment

4 Conclusion

In this report, the motion of an 8 bar mechanism was examined. The purpose of the mechanism is to move a rod parallel to another rod, while extending horizontally. In this research, the kinematic and dynamic analysis were performed. The kinematic analysis yielded the position, velocity and acceleration of the mechanism. To ensure that these calculations were correct, they have been checked in several ways. The dynamic analysis resulted in the forces in each bar and the driving moment. These were also checked, to ensure accuracy.